

Intracellular Zinc Depletion Induces Caspase Activation and p21^{Waf1/Cip1} Cleavage in Human Epithelial Cell Lines

F. Chai,^{1,a} A. Q. Truong-Tran,^{1,a} A. Evdokiou,²
G. P. Young,³ and P. D. Zalewski¹

¹Department of Medicine, University of Adelaide, Queen Elizabeth Hospital, Woodville, ²Department of Orthopaedics and Trauma, University of Adelaide, Royal Adelaide Hospital, Adelaide, and ³Department of Medicine, Flinders University of South Australia, Bedford Park, South Australia

To better understand the mechanisms by which zinc deficiency induces epithelial cell death, studies were done of the effects of intracellular zinc depletion induced by the zinc chelator TPEN on apoptosis-related events in human malignant epithelial cell lines LIM1215 (colonic), NCI-H292 (bronchial), and A549 (alveolar type II). In TPEN-treated cells, depletion of zinc was followed by activation of caspase-3 (as demonstrated by enzymatic assay and Western blotting), DNA fragmentation, and morphologic changes. Increase in caspase-3 activity began 1–2 h after addition of TPEN, suggesting that zinc may suppress a step just before the activation of this caspase. Caspase-6, a mediator of caspase-3 processing, also increased, but later than caspase-3. Effects of TPEN on apoptosis were completely prevented by exogenous ZnSO₄ and partially prevented by peptide caspase inhibitors. A critical substrate of caspase-3 may be the cell cycle regulator p21^{Waf1/Cip1}, which was rapidly cleaved in TPEN-treated cells to a 15-kDa fragment before further degradation.

The group IIb zinc metal is an important factor in resistance to infectious agents as evident from the increased rates of infections in zinc-deficient animals and humans (reviewed in 1–3). Zinc may mediate resistance to infection at two levels: first, via a beneficial effect on the immune system where it promotes the survival, proliferation, and function of T cells, especially the Th1 subset; and, second, by protecting the epithelial tissues from damage by oxidants and other noxious agents, thereby facilitating innate immunity. Zinc deficiency can result in epithelial lesions in the skin and gastrointestinal lining [4] and a heightened susceptibility to damage by other toxins (e.g., in the duodenum by colchicine [5]). One of the mechanisms of zinc deficiency-induced epithelial damage is by increased death of epithelial cells via the cell suicide process of apoptosis (gene-directed cell death) [6]. Zinc deficiency can also result in cell death by necrosis, especially if the apoptotic pathway is dysfunctional [7]. The mechanisms by which zinc deficiency enhances apoptosis remain unclear. Therefore, in this study, we attempted to better understand these mechanisms by using a variety of epithelial cell lines induced to apoptose by *in vitro* zinc deprivation.

A variety of antiapoptotic and proapoptotic proteins interact

to regulate the pathways of apoptosis in cells. Among the major proapoptotic proteins is the caspase family of aspartate-specific proteases [8]. The caspase family of effector enzymes has been implicated in many [8], although not all [9], biochemical pathways leading to apoptosis. Among the caspase-dependent forms of apoptosis, three major pathways have been described [10, 11]. The first involves membrane receptor-ligand interactions (e.g., Fas-FasL binding) and results in activation of the upstream caspase, caspase-8; the second pathway, often triggered by chemical stimuli, causes changes in mitochondrial membrane permeability, release of cytochrome c into the cytoplasm, and subsequent activation of the upstream caspase, caspase-9; a third pathway involves caspase-12 and is triggered in response to stress-induced changes in the endoplasmic reticulum [11].

Both caspase-8 and caspase-9 trigger, indirectly or directly, activation of the major effector caspase, caspase-3/DEVD-caspase. This caspase-3 in turn cleaves after DXXD in poly (ADP-ribose) polymerase and other substrates, triggering the distinctive biochemical and morphologic changes associated with this apoptotic cell death [8]. Hence, the detection of this enzyme is critical and has led to the development of an enzymatic assay, based on liberation of a fluorogenic coumarin derivative AFC from the substrate DEVD-AFC [12]. Caspase-3 is activated by cleavage of a 32-kDa zymogen (CPP32); cleavage results in the formation of large and small subunits that rearrange to form an active caspase [12]. Cleavage of the precursor form of caspase-3 is mediated by other caspases, especially caspase-9 and caspase-6 (previously known as Mch2 α [13]). Caspase-9-dependent cleavage of CPP32 is triggered by the release of cytochrome c from mitochondria and is suppressed by Bcl-2 [10, 14]. The factors regulating caspase-6 cleavage of CPP32 are

Financial support: Overseas Postgraduate Research Scholarship (to F.C.); University of Adelaide Benjamin Poulton Scholarship (to A.Q.T.-T.).

^a F.C. and A.Q.T.-T. are equal first authors of this work.

Reprints or correspondence: Dr. P. D. Zalewski, Dept. of Medicine, University of Adelaide, Queen Elizabeth Hospital, Woodville, South Australia 5011 (pzalewski@medicine.adelaide.edu.au).

unknown. Therefore the biochemical pathways governing the activation and processing of these caspases are a subject of much interest.

Our laboratory [15] and others [16–18] recently identified one of these targets as the universal cell cycle regulator p21^{Waf1/Cip1}. p21 is an inhibitor of various members of the cyclin-dependent kinases (CDKs), which control the orderly progression of cells through different cell cycle states [19]. p21 contains a domain near its amino terminus that binds to cyclin/CDK complexes; this interaction inhibits CDK activity and hinders its ability to phosphorylate the retinoblastoma family of proteins. This, in turn, is responsible for G₁/S phase arrest induced by p53 in response to DNA damage [19]. In addition to its N-terminal CDK inhibitory domain, p21 contains a proliferating cell nuclear antigen (PCNA) binding motif located in the carboxy terminal part of the protein that may be important for the inhibition of DNA replication by p21 [20]. Recently, the cleavage of p21 by a caspase-3–like activity during apoptosis in response to various stimuli was reported. These include cleavage of p21 in butyrate-treated LIM1215 cells [15], tumor necrosis factor–induced apoptosis of human cervical carcinoma cells [16], and growth factor–deprived human endothelial cells [16] in response to DNA damage by γ -irradiation and DNA-damaging agents [18].

Here we sought to determine whether depletion of intracellular zinc in various epithelial cell lines would influence activation of caspase-3 and caspase-6 and the cleavage of p21. We used three human malignant epithelial cell lines: colonic epithelial LIM1215 cells, bronchial epithelial NCI-H292 cells, and alveolar type II epithelial A549 cells. These cell lines have been widely used in our laboratory to dissect the biochemical pathways regulating apoptosis induced by various agents [21]. Intracellular zinc was depleted by use of the membrane-permeable zinc chelator TPEN [22], and levels of this zinc were monitored with a UV-excitable intracellular zinc (II)-specific fluorophore, Zinquin [21, 22].

Methods and Materials

Materials. Major materials and their suppliers were: EDTA, EGTA, herring sperm DNA, Nonidet P-40 (NP-40), dithiothreitol (DTT), sucrose, HEPES (Sigma Chemical, St. Louis); complete protease inhibitor cocktail (Boehringer Mannheim, Mannheim, Germany); penicillin/streptomycin, EDTA/trypsin, RPMI 1640 culture medium, glutamine, CHAPS (ICN, Aurora, OH); gentamicin (David Bull Laboratories, Melbourne); Coomassie brilliant blue G-250 (BDH, Sydney); fetal bovine serum (FBS; Biosciences, Sydney); zDEVD-AFC, zVAD-fmk, zDEVD-fmk (Kamiya Biomedical, Tukwila, WA); VEID-AFC (Calbiochem NSW, Alexandria, Australia); Zinquin, ethyl-[2-methyl-8-*p*-toluenesulphonamido-6-quinolyloxy]acetate [23] was obtained from A. D. Ward, Department of Chemistry, University of Adelaide, South Australia, dissolved in DMSO as a 5 mM stock solution and stored in aliquots

at –20°C in the dark. All other reagents were reagent grade, unless indicated.

Cell cultures. LIM1215 cells were obtained from R. Whitehead (Ludwig Institute, Melbourne), while A549 and NCI-H292 cells were obtained from D. Knight (QEII Medical Centre, Perth, Western Australia). Cell lines were cultured in RPMI 1640, buffered in HEPES at pH 7.4, and supplemented with glutamine (2 mM), penicillin (100 IU/mL), streptomycin (100 μ g/mL), gentamicin (160 μ g/mL), and 10% FBS in a humidified atmosphere containing 5% CO₂. Experiments were performed either in 25-cm² vented tissue culture flasks or 6-well plates (Sarstedt, Newton, NC). Cells were allowed to attach and grow for 2–3 days to confluence prior to exposure to test reagents. TPEN was added from a stock solution of 5 mM in DMSO to give the final indicated concentration. The final concentration of DMSO was \leq 0.5% after addition of TPEN.

Quantification of Zinquin fluorescence by image analysis. Cells were grown to semiconfluence on sterile glass coverslips in 6-well plates for 48 h before the addition of Zinquin. Coverslips were then washed in PBS and incubated with 25 μ M Zinquin in PBS for 30 min at 37°C. Coverslips were inverted on microscope slides. Fluorescence was examined by a microscope (BH2; Olympus, Tokyo) equipped with epifluorescence, UV B dichroic mirror for low wavelength excitation, and connected to a Panasonic CCTV video color camera suitable for low light fluorescence with integration capabilities and a computer work station. Both fluorescence images and corresponding phase contrast microscope images were captured and stored using a 20 \times objective lens. With the VideoPro (Leading Edge) image analysis system, lines were drawn around the borders of cells, and fluorescence intensity within the borders was measured. For all images, background illumination in an area not occupied by cells was subtracted from the readings.

Apoptotic DNA fragmentation. To assay DNA fragmentation, cells (5×10^6 – 10^7 in total) were lysed at 4°C in 1 mL of NP-40 lysis buffer (5 mM Tris-HCl, pH 7.5, containing 5 mM EDTA and 0.5% NP-40) and centrifuged at 13,000 *g* for 10 min at 4°C. Supernatant fractions containing low-molecular-weight DNA fragments were assayed for DNA by a fluorometric technique [24]. Hoechst dye 33258 was dissolved in deionized water to a concentration of 1 mg/mL and stored at 4°C. Prior to use, 1 μ L of dye was added per 10 mL of buffer (10 mM Tris-HCl, pH 7.4, containing 1 mM EDTA and 100 mM NaCl). Aliquots of lysate (20–50 μ L) were placed into fluorimeter-grade disposable cuvettes (Greiner, Kremsmunster, Austria) and 1 mL of diluted dye solution was added. Fluorescence was measured at an excitation wavelength of 356 nm and emission wavelength of 458 nm (slit widths, 10 nm) in a fluorescence spectrophotometer (LS50; Perkin-Elmer, Norwalk, CT). Herring sperm DNA was used to derive a standard curve.

Measurement of DEVD-caspase (caspase-3) and VEID-caspase (caspase-6) activities. DEVD-caspase was assayed by cleavage of DEVD-AFC (asp-glu-val-asp-7-amino-4-trifluoro-methyl-coumarin), a fluorogenic substrate based on the peptide sequence at the caspase-3 cleavage site of poly (ADP-ribose) polymerase [12]. VEID-caspase was assayed by cleavage of VEID-AFC (val-glu-ile-asp-7-amino-4-trifluoro-methyl-coumarin), a fluorogenic substrate based on the peptide sequence at the caspase-6 cleavage site of lamin [13]. Cells (5×10^6 – 10^7 per flask) were cultured with test reagents, washed once with 5 mL of HBSS, and resuspended in 1

mL of NP-40 lysis buffer (as for DNA fragmentation). After 15 min in lysis buffer at 4°C, insoluble material was pelleted at 15,000 *g* and an aliquot of the lysate was tested for protease activity. To each assay tube, we added 10–20 μ L of cell lysate and then 1 mL of protease buffer (50 mM Hepes, 10% sucrose, 10 mM DTT, 0.1% CHAPS, pH 7.4) containing 8 μ M of substrate. After 4–18 h at room temperature, fluorescence was quantified (excitation 400, emission 505) in the LS50 spectrofluorometer. Optimal amounts of added lysate and duration of assay were taken from linear portions of curves as determined in preliminary experiments. One unit of caspase activity was considered to be 1 fluorescence U (at slit widths of 5 nm) per microgram of lysate protein.

Flow cytometric assay for apoptosis. Cells were removed from culture dishes by trypsinization, collected by centrifugation, resuspended in ice-cold PBS, and fixed in absolute methanol for \geq 30 min. Cells were then washed in PBS containing 0.5% Tween 20, followed by two washes in PBS containing 2% fetal calf serum (FCS). After the washes, cells were resuspended in PBS/2% FCS containing 40 μ g/mL RNase A and incubated for 20 min at 37°C. Finally, cells were washed in PBS/2% FCS and resuspended in PBS containing propidium iodide (20 μ g/mL). The stained nuclei were analyzed by flow cytometer (Epics Profile; Coulter, Hialeah, FL). Cell cycle distribution was based on 2N and 4N DNA content. Cells with $<$ 2N DNA content were indicative of apoptotic cells. A linear measurement scale was used for quantification.

Morphologic assessment of apoptosis. Apoptosis was also assessed in some experiments by chromatin condensation in hematoxylin eosin (HE)-stained cell cultured coverslips and by labeling of nuclear fragments with Hoechst dye 33258 (1 μ g/mL). One thousand cells were scored from replicate tubes.

Protein assay. Protein concentration was measured by the DC protein assay kit (BioRad Laboratories, Hercules, CA) in accordance with the manufacturer's instructions.

Western blotting. Cell aliquots were lysed in NP-40 lysis buffer (5 mM Tris-HCl, pH 7.5, containing 5 mM EDTA, 0.5% NP-40, and complete protease inhibitor cocktail) and stored at -20° C until assayed. One volume of 4 \times SDS-loading buffer (250 mM Tris-HCl, pH 6.8, 40% [vol/vol] glycerol, 8% [wt/vol] SDS, 20% [vol/vol] 2-mercaptoethanol, and 0.5% [wt/vol] bromophenol blue) was added to three volumes of lysate and mixtures were denatured. Equal protein amounts (18–36 μ g) were loaded into wells and electrophoresed on 12% minigels (Bio-Rad) at 200 V for 45 min. To ensure that equal amounts of protein were loaded in each track, duplicate gels were also stained with Coomassie brilliant blue G-250. Proteins were blotted onto Immobilon-P polyvinylidene difluoride membrane (Millipore, Sydney). Membranes were pre-blocked with 3% powdered milk in Tris-buffered saline/0.1% Tween 20 and 3% bovine serum albumin for 60 min at room temperature.

Primary antibodies used were mouse monoclonal anti-human p21 (clone 6B6, 1/333 dilution; PharMingen, San Diego), goat polyclonal anti-human Mch2 p20 (K-20) IgG (1/500 dilution, Santa Cruz Biotech, Santa Cruz, CA) and goat polyclonal anti-human CPP32 p20 (N-19) IgG (1/1000 dilution, Santa Cruz Biotech). Secondary antibody was either sheep anti-mouse IgG peroxidase conjugate (1/1000 dilution, Fab fragment; Boehringer Mannheim) or anti-goat IgG peroxidase conjugate (1/1000 dilution, whole antibody, Santa Cruz Biotech). Primary antibodies were added for 60 min and secondary antibodies for 45 min at room temperature.

Membranes were then soaked in enhanced chemiluminescence Western blotting reagent (Amersham Life Sciences, Sydney), and bands were detected by chemiluminescence. Rainbow high-molecular-weight markers (Amersham Life Sciences) were used for determination of molecular weight.

Experimental design. All experiments were repeated a minimum of three times. Statistical significance was determined by Student's *t* test and as indicated in text or figure legends.

Results

Intracellular zinc depletion by TPEN as demonstrated by decrease in Zinquin fluorescence. In order to deplete intracellular zinc, cell lines were treated with varying concentrations of the membrane-permeable zinc chelator TPEN. Intracellular zinc content (specifically the more labile pools of zinc) were monitored by loading the cells with the zinc-specific fluorophore Zinquin. Figure 1 shows the strong quenching of Zinquin fluorescence by TPEN in two of these cell lines, A549 (upper panels) and NCI-H292 (lower panels). The panel on the right in figure 1 represents the normal zinc content of the cells, while the panels on the left show the zinc-depleted cells after addition of TPEN for 1 h. Zinquin fluorescence was significantly quenched by TPEN, which has a much higher affinity for zinc than Zinquin [22]. Thus, in NCI-H292 cells, specific mean fluorescence intensity decreased from 23.1 ± 2.2 pixels ($n = 29$)

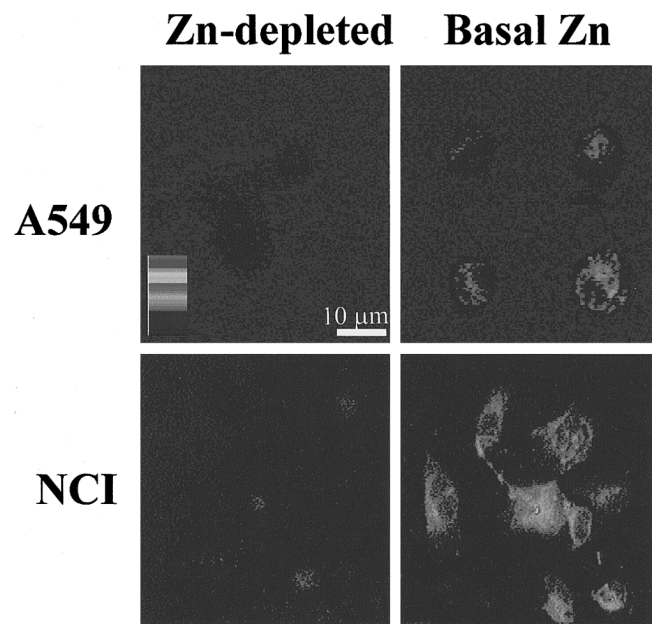


Figure 1. Depletion of zinc (Zn) in epithelial cells as shown by Zinquin fluorescence. Images of Zinquin fluorescence of intracellular zinc in A549 (upper panels) and NCI-H292 cells (lower panels). Right panels demonstrate basal Zinquin fluorescence of untreated cells (weak for A549 and moderate for NCI-H292 cells). Left panels show quenched fluorescence following intracellular zinc depletion using TPEN. Note linear color scale of 0–255 pixels.

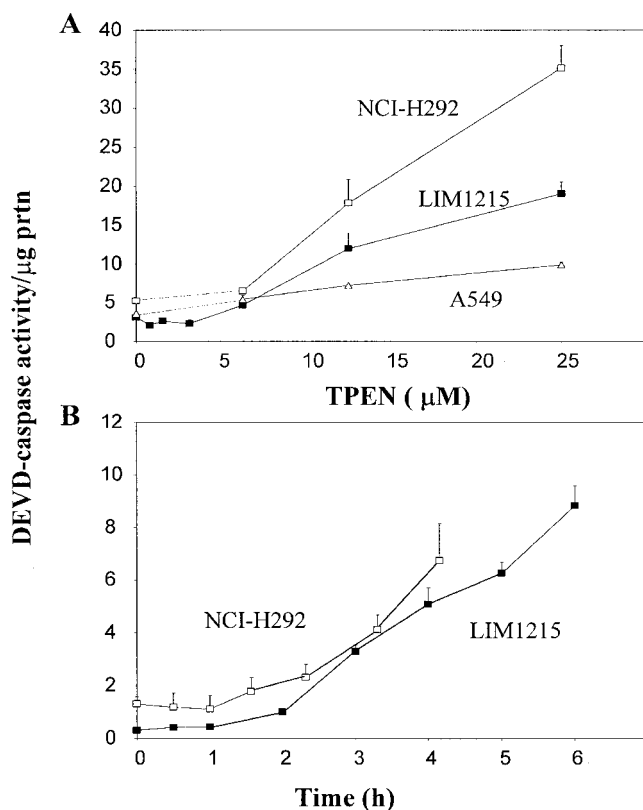


Figure 2. TPEN-induced activation of DEVD-caspase activity. *A*, LIM 1215 cells were treated with varying concentrations of TPEN for 3 h (■); other cell lines were treated for 4 h (A549, △; NCI-H292, □). *B*, Cells were treated for varying times with 25 μM TPEN. Cell lysates were assayed for DEVD-caspase activity. Typical experiment is shown for LIM1215 and NCI-H292 cells. Data are means of triplicates; error bars indicate SDs. For A549 and NCI-H292 cells, data were collated from 3 experiments, each in triplicate.

in cells incubated with Zinquin alone to 9.7 ± 0.7 pixels ($n = 28$) in cells incubated with Zinquin + 25 μM TPEN ($P \leq .005$); in A549 cells, fluorescence decreased from 11.8 ± 0.3 pixels ($n = 192$) in cells incubated with Zinquin alone to 7.2 ± 0.3 pixels ($n = 187$) in cells incubated with Zinquin + 25 μM TPEN ($P \leq .05$).

Zinc depletion induces caspase-3 activation and DNA fragmentation. To determine the effects of zinc depletion on caspase-3 activation, epithelial cells were treated with varying concentrations of TPEN for 4 h. Cell lysates were prepared and assayed for DEVD-caspase activity (figure 2*A*). In each of the three cell lines, there was a significant increase in DEVD-caspase activity, especially at TPEN concentrations ≥ 12.5 μM. Thus, in LIM1215 cells (figure 2*A*), there was a small but significant ($P \leq .05$) increase in DEVD-caspase activity with 6.25 μM TPEN, followed by highly significant increases ($P \leq .005$) at 12.5 and 25 μM TPEN (the latter yielding a maximal response).

The kinetics of these increases were studied using 25 μM TPEN. DEVD-caspase activity increased slowly between 1 and 2 h after addition of TPEN in both cell lines studied (NCI-H292 and LIM1215, figure 2*B*). After 2 h, there were sharp rises in DEVD-caspase activity, increasing linearly up to 6 h (the latest time point tested). The induction of DEVD-caspase activity by TPEN was prevented at all time points when cells also received exogenous ZnSO₄ (25 μM). Thus, after 5 h of TPEN treatment in LIM1215 cells (figure 2*B*), there was an increase in DEVD-caspase activity over the control (no TPEN) of 5.9 U/μg of protein. Similarly, for NCI-H292 cells (figure 2*B*), there was a corresponding increase of 5.4 U/μg of protein. When LIM1215 cells were treated with TPEN in the presence of 25 μM of ZnSO₄, there was a 10-fold reduction to 0.4 U/μg of protein. Since TPEN can also chelate copper and nickel, it is possible that some of the responses were due to chelation of these metal ions. However, our zinc supplementation studies demonstrated that TPEN was acting by chelating zinc.

The fluorogenic substrate assays, which showed an increase in DEVD-caspase activity in TPEN-treated cells, could indicate rises in caspase-3 or caspase-7, both of which can cleave this substrate. The Western blot in figure 3 confirmed that TPEN induced caspase-3 activity, as determined by the decrease in the 32-kDa zymogen form (CPP32) of caspase-3. The antibody used in this blot failed to pick up either of the active subunits of caspase-3, probably due to the specificity of the antibody used. The decrease in CPP32 was most evident between 2 and 3 h after addition of TPEN (figure 3*A*), consistent with the results of the fluorogenic substrate assay (figure 2*B*).

Zinc depletion by TPEN induces caspase-6 activation. CPP32 can be processed to its active form by other caspases,

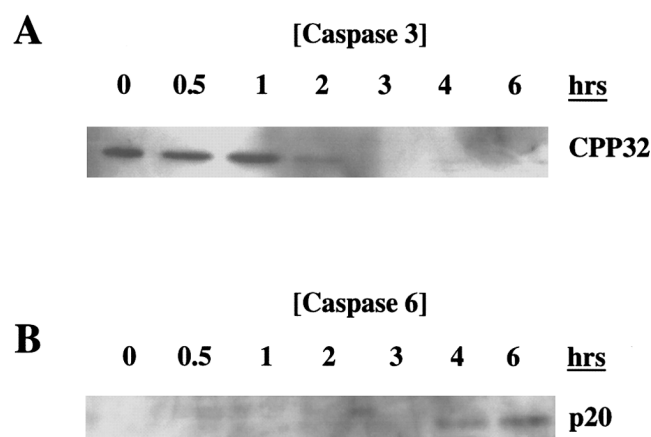


Figure 3. TPEN-induced activation of caspase-3 and caspase-6 by Western blotting. LIM1215 cells were treated with 25 μM TPEN for varying times (≤ 6 h). Cell lysates were prepared and assayed for caspase-3 (*A*) or caspase-6 (*B*) by Western blotting. Antibody for caspase-3 detected only 32-kDa precursor (CPP32). Antibody for caspase-6 detected the active p20 subunit. Typical experiments are shown.

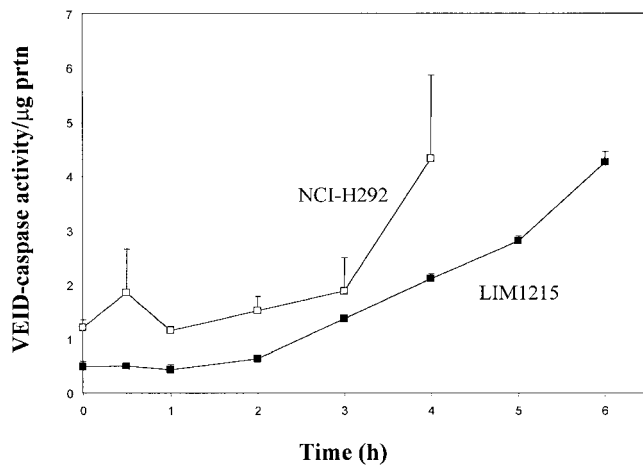


Figure 4. Induction of caspase-6 enzymatic activity in TPEN-treated cells. LIM1215 or NCI-H292 cells were treated with 25 μ M TPEN for varying periods (≤ 6 h). Cell lysates were prepared and assayed for caspase-6 activity with the fluorogenic substrate VEID-AFC. Data are means of triplicates. Error bars indicate SDs. Typical experiments are shown.

including caspase-6. To determine whether TPEN is activating caspase-3 by inducing caspase-6, LIM1215 or NCI-H292 cells were treated with 25 μ M TPEN for varying periods. Caspase-6 activity was monitored by Western blotting to detect the active p20 subunit (figure 3B) or by a fluorogenic substrate assay with VEID-AFC. The active p20 subunit of caspase-6 did not increase significantly in the first 2 h after addition of TPEN to LIM1215 cells but increased steadily after 2 h (figure 3B). Similar results were obtained by the enzymatic assay, with increases in VEID-caspase occurring after 2 h in LIM1215 cells and after 3 h in NCI-H292 cells (figure 4). These observations suggest that caspase-6 is not significantly involved in the activation of caspase-3 in zinc-depleted epithelial cells.

Zinc depletion induces DNA fragmentation and apoptosis. Effects on apoptosis were determined by measuring DNA fragmentation and by flow cytometry. Data are shown for LIM1215 cells. DNA fragmentation induced by TPEN displayed a similar dependence on concentration (figure 5A) and time (figure 5B) to that of DEVD-caspase activation. The first increase in DNA fragmentation occurred after 2 h and a large increase occurred after 3 h and was almost linear up to 6 h. Flow cytometry analysis with propidium iodide showed a progressive increase in apoptotic cells, as indicated by appearance of an increasing fraction of cells with less than 2N DNA content, preceding the G₁ peak on the fluorescence scans (figure 6). Cells containing hypodiploid DNA increased 1 h after addition of TPEN and plateaued at 3 h. The discordance between DNA fragmentation (figure 5B) and flow cytometry (figure 6) for apoptosis may be due to the presence of necrotic cells and differences between processing techniques for the two assays. When observed mi-

croscopically, cells treated with TPEN had chromatin condensation (as determined by HE staining), nuclear fragmentation (as determined by Hoechst dye 33258), and formation of distinct apoptotic bodies consistent with apoptosis (not shown).

Caspase inhibitors block TPEN-induced caspase-3 activation but only partially block DNA fragmentation. To determine whether caspases are involved in the subsequent apoptosis of TPEN-treated epithelial cells, two specific membrane-permeable peptide inhibitors of caspase-3 were used. zDEVD-fmk is a specific inhibitor of caspase-3, while zVAD-fmk is an inhibitor of a broad spectrum of caspases [10]. Both inhibitors completely inhibited DEVD-caspase activity in TPEN-treated LIM1215 cells (figure 7A), although it was not determined whether the peptide inhibitors blocked the active caspase-3 or the caspase-dependent steps leading to activation of caspase-3. Despite the complete inhibition of DEVD-caspase activity, there was only partial inhibition of DNA fragmentation, even at higher concentrations of inhibitors (figure 7B). Hence DNA fragmentation in zinc-depleted cells was partially caspase independent.

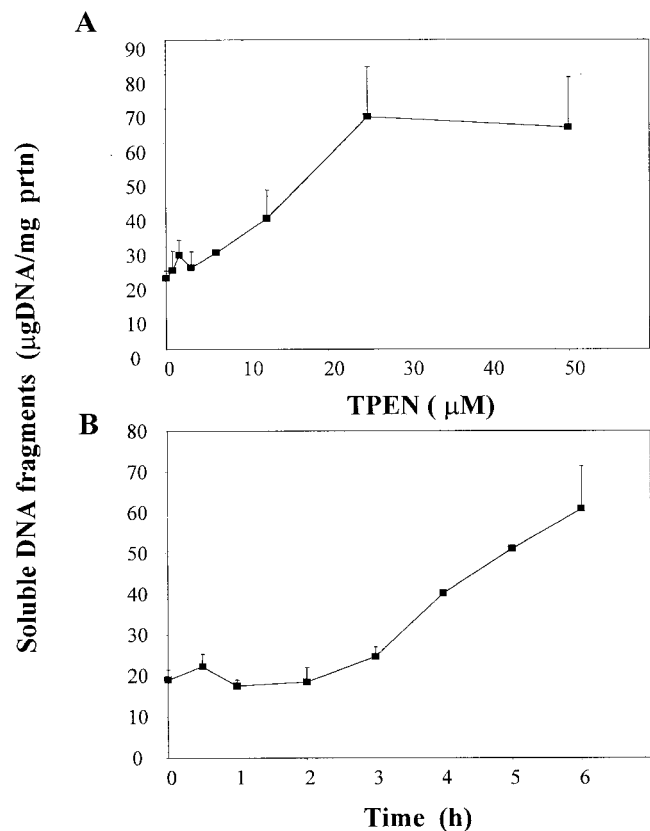


Figure 5. TPEN-induced DNA fragmentation. LIM1215 cells were treated with varying concentrations of TPEN for 3 h (A) or for varying times with 25 μ M TPEN (B). Lysates were assayed for soluble DNA fragments. Typical experiment is shown. Data are means of triplicates. Error bars indicate SDs.

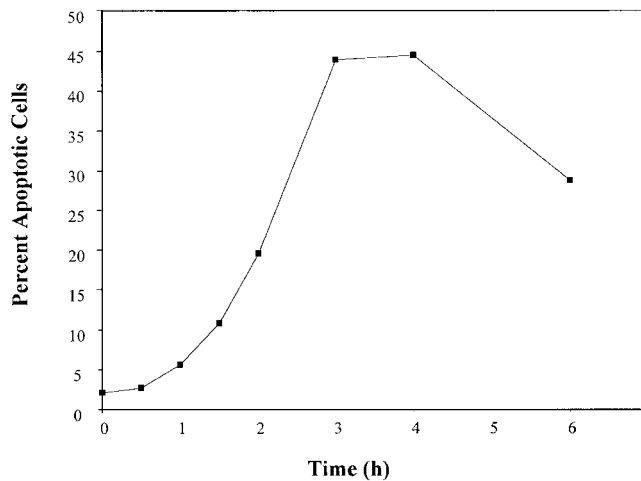


Figure 6. TPEN-induced apoptosis measured by flow cytometry. LIM1215 cells were treated for varying times with 25 μ M TPEN. Combined nonadherent and adherent cell populations were washed, fixed, and analyzed by flow cytometry (see Materials and Methods). Percent “sub-G1” apoptotic cells are shown on y axis.

Although the level of DNA fragmentation in cells treated with zVAD-fmk appeared to be higher than in control cells, there was no statistically significant increase ($P > .05$).

TPEN induces loss of p21 associated with appearance of p15 and eventually loss of both species. Previous studies from our laboratory and others identified the cell cycle regulator p21 as a specific substrate of caspase-3 in cells induced to apoptose by butyrate and other agents [15–18]. We therefore determined whether p21 was also cleaved in zinc-depleted cells. LIM1215 cells were treated with 25 μ M TPEN for varying time periods, and lysates were assayed by Western blotting with a p21 monoclonal antibody. This antibody also detected the larger p15 cleavage product of p21 formed by caspase-3–dependent cleavage of p21 at D₁₁₂. Decrease in p21 and appearance of p15 first occurred 1 h after addition of TPEN (figure 8, track B). By 2 h, most of the p21 had been cleaved, and there was a major band corresponding to p15. By 4 h, neither p21 nor p15 were detectable, suggesting further degradation of p15. Similar results were obtained for the other cell line tested (A549) (data not shown).

Effects on p21 are mediated, at least in part, by caspase-3 cleavage. A comparison of the time courses of caspase-3 activation and p21 degradation in TPEN-treated cells suggests that p21 loss is mediated by caspase-3. To investigate this further, LIM1215 cells were pretreated with zDEVD-fmk (0–100 μ M) for 1 h before the addition of 25 μ M TPEN for a further 2 h. Lysates were then prepared and assayed by Western blotting with p21. At 50 and 100 μ M zDEVD-fmk, there was complete suppression of cleavage of p21 to p15 (data not shown).

Discussion

Enhanced apoptotic cell death in epithelial tissues is a consequence of in vivo zinc deficiency and may play an important role in the formation of the characteristic vesicular skin lesions [25], damage to the gastrointestinal lining and associated diarrhea [26], and sloughing of the respiratory epithelium. This study addressed the mechanisms by which depletion of intracellular zinc induces apoptosis of epithelial cells by use of an in vitro model in which human malignant epithelial cell lines were treated with the zinc chelator TPEN. This study had three major conclusions: Apoptosis in zinc-depleted cells proceeds via a caspase-3–dependent process, there is only a short lag period (1–2 h) between addition of TPEN and onset of caspase-3 activation, and activation of caspase-3 is rapidly followed by loss of p21^{Waf1/Cip1}, first to a 15-kDa fragment and then further degraded.

Our findings in TPEN-treated cells of (first) an increase in DEVD-caspase activity, (second) loss of the 32-kDa zymogen form of caspase-3, and (third) partial suppression of DNA frag-

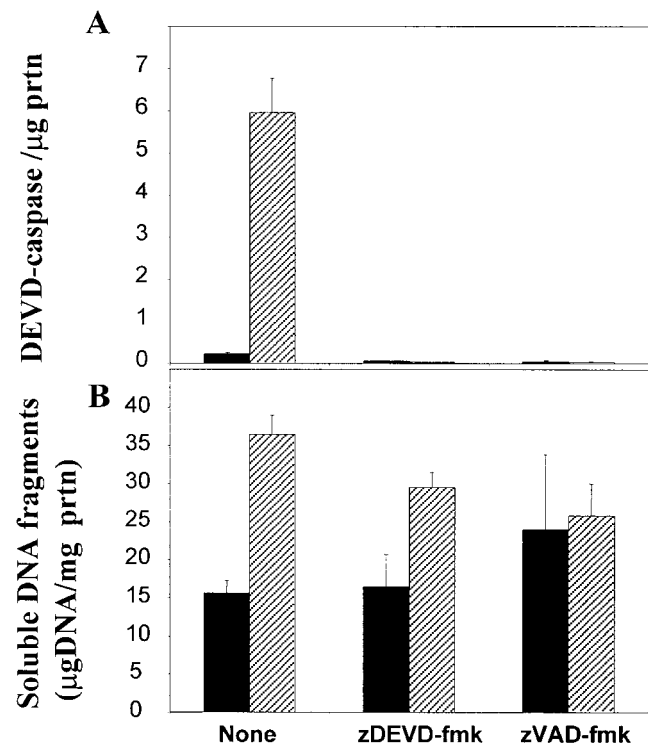


Figure 7. Effects of caspase peptide inhibitors on DEVD-caspase activity and DNA fragmentation. LIM1215 cells were pretreated for 1 h with 10 μ M zDEVD-fmk or 25 μ M zVAD-fmk before addition of 0 (solid columns) or 25 μ M (hatched columns) TPEN for another 3.5 h. Cell lysates were prepared and assayed for DEVD-caspase activity (A) or soluble DNA fragments (B). Data are means of triplicates from typical experiment; error bars indicate SDs. Significance was determined by Student's *t* test. prt/n, protein.

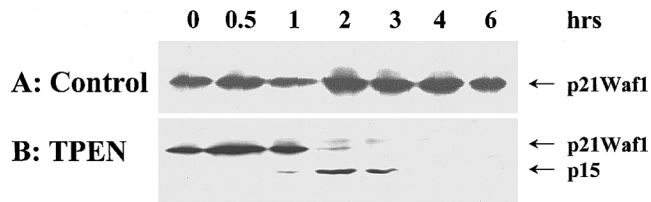


Figure 8. Effect of zinc depletion on p21 cleavage. LIM1215 cells were treated in absence (*A*) or presence (*B*) of 25 μ M TPEN for varying time periods. Effects on p21 were determined by Western blotting. Typical experiment is shown. Position of p21 and cleaved fragment p15 are indicated by arrows.

mentation by caspase peptide inhibitors (including a specific inhibitor of caspase-3, zDEVD-fmk), argue for a major role of caspase-3 in the TPEN-induced apoptosis. This conclusion is strengthened by the recent study of TPEN-induced cell death in human renal cell carcinoma cell lines, in which mutant cell lines lacking caspase-3 were resistant to TPEN-induced apoptosis [7]. Since these resistant cell lines also had variable decreases in caspase-7, -8, and -10, it cannot be ruled out that loss of one of these upstream caspases may also have been important. Caspase-6, the caspase responsible for cleavage of nuclear lamins [13], was also activated in zinc-depleted cells in our study, and this caspase may be responsible for the subsequent nuclear fragmentation in zinc-depleted cells. Suppression of TPEN-induced DNA fragmentation by the caspase-3 peptide inhibitor zDEVD-fmk was only partial, despite complete suppression of DEVD-caspase activity. That other caspases may substitute for caspase-3 is unlikely since the broad-spectrum caspase inhibitor zVAD-fmk was also only partially able to suppress DNA fragmentation. We believe that at least some of the resulting DNA fragmentation is via a caspase-independent mechanism, although whether DNA fragmentation also occurs by nonapoptotic mechanisms cannot be ruled out. The observations that TPEN lowers intracellular zinc under the conditions used in this study and that zinc supplementation prevents the effects of TPEN on apoptosis of these cells, suggests that depletion of zinc is responsible for most, if not all, of the actions of TPEN on these cells.

We recently reported on the importance of zinc as a regulator of apoptosis [27]. The mechanism by which intracellular zinc depletion triggers caspase-3 activation remains unclear. In view of the short lag period (1–2 h) between addition of TPEN and onset of caspase-3 activation, zinc must influence a step relatively close to that of caspase-3 activation. Indeed, in primary tracheobronchial ciliated epithelial cells, zinc is concentrated in the apical cytoplasm [28], the same region in which the precursor form of caspase-3 is localized [29]. Caspase-3 activation involves the proteolytic processing of a 32-kDa zymogen by other caspases; both caspase-9 [14] and caspase-6 [30] have been implicated in this processing. It is of interest that both of these

caspases are very sensitive to inhibition by zinc [13, 31, 32]. TPEN might therefore act by stripping zinc from either or both of these caspases, thus enhancing their activity. We were unable to show any significant activation of caspase-6 prior to activation of caspase-3. Caspase-6 was activated in TPEN-treated cells, but only at time points later than that of caspase-3 activation. It is possible that only small amounts of caspase-6 are required for processing of caspase-3 and that these levels were too low to be detected by our fluorogenic substrate assay. Effects of zinc depletion on caspase-9 activity now need to be determined. Alternatively, zinc may influence the levels of auxiliary factors in the activation of caspase-3. Candidates include members of the Bcl-2 family of proteins, which suppress caspase-3 activation and may be up-regulated by zinc supplementation [33]. Another candidate may be nitric oxide, since a nitric oxide synthase inhibitor protects mice from zinc deficiency-induced apoptosis and damage in the gastrointestinal epithelium [34].

The third major conclusion of this study is that activation of caspase-3 in zinc-depleted cells is rapidly followed by loss of the cell-cycle regulator p21^{Waf1/Cip1}. This loss occurs in two steps: Initially, there is cleavage of p21 to a 15-kDa derivative, which we [14] and others [15–17] have shown to arise by caspase-3-dependent cleavage of p21 at D₁₁₂. This cleavage, which separates the N-terminal domain (that binds to and inhibits the cyclin-cdk complex) from the C-terminal (that binds to the nuclear proliferation-associated marker PCNA), results in a 15-kDa fragment that cannot localize in the nucleus but facilitates apoptosis by poorly understood mechanisms. After the initial cleavage of p21, there was complete loss in zinc-depleted cells. Since the turnover of p21 is regulated by the proteasome complex of proteases [35], the initial cleavage to p15 may expose sites that facilitate ubiquitination and subsequent targeting to the proteasome. Loss of p21 may result in premature entry of the cells into S-phase, and apoptotic cell death occurs in some other forms of apoptosis [36]. Experiments to test the effect of zinc depletion on apoptosis in cells transfected with a mutant form of p21 that has an alanine instead of aspartate at position 112 and which will, therefore, be resistant to caspase-dependent cleavage, should prove informative.

The extent to which in vivo zinc deficiency is associated with enhanced rates of caspase activation, p21 degradation, and apoptosis in epithelial tissues needs to be determined. This will best be answered in the context of experimental zinc deficiency in animals that will allow these parameters to be correlated with impaired barrier function and increased rates of infections.

Acknowledgments

We acknowledge Bob Whitehead for supplying the colorectal cancer cell line LIM1215 and Philip Thompson and Darryl Knight for supply of A549 and NCI-H292 cells. We also thank Belinda Farmer for assistance with flow cytometry analysis.

References

- Zalewski PD. Zinc and Immunity: implications for growth, survival and function of lymphoid cells. *J Nutr Immun* **1996**;4:39–101.
- Shankar AH, Prasad AS. Zinc and immune function: the biological basis of altered resistance to infection. *Am J Clin Nutr* **1998**;68(suppl 2):447S–63S.
- Walsh CT, Sandstead HH, Prasad AS, Newberne PM, Fraker PJ. Zinc: health effects and research priorities for the 1990s. *Environ Health Perspect* **1994**;102(suppl 2):5–46.
- Solomons NW. Zinc and copper. In Shils ME, Young VR, eds. *Modern nutrition in health and disease*, 7th ed. Philadelphia: Lea and Febiger, **1988**:238–62.
- Dinsdale D, Williams RB. The enhancement by dietary zinc deficiency of the susceptibility of the rat duodenum to colchicine. *Br J Nutr* **1977**;37:135–42.
- Zalewski PD, Forbes IJ. Intracellular zinc and the regulation of apoptosis. In: Lavin M, Watters D, eds. *Programmed cell death: the cellular and molecular biology of apoptosis*. Melbourne: Harwood Academic Publishers, **1993**:73–86.
- Kolenko V, Uzzo RG, Bukowski R, et al. Dead or dying: necrosis versus apoptosis in caspase-deficient human renal cell carcinoma. *Cancer Res* **1999**;59:2838–42.
- Thornberry NA, Lazebnik Y. Caspases: enemies within. *Science* **1998**;281:1312–6.
- Chautan M, Chazal G, Cecconi F, Gruss P, Golstein P. Interdigital cell death can occur through a necrotic and caspase-independent pathway. *Curr Biol* **1999**;9:967–70.
- Sun XM, MacFarlane M, Zhuang J, Wolf BB, Green DR, Cohen GM. Distinct caspase cascades are initiated in receptor-mediated and chemical-induced apoptosis. *J Biol Chem* **1999**;274:5053–60.
- Nakagawa T, Zhu H, Morishima N, et al. Caspase-12 mediates endoplasmic-reticulum-specific apoptosis and cytotoxicity by amyloid-beta. *Nature* **2000**;403:98–103.
- Nicholson DW, Ali A, Thornberry NA, et al. Identification and inhibition of the ICE/CED-3 protease necessary for mammalian apoptosis. *Nature* **1995**;376:37–43.
- Takahashi A, Alnemri ES, Lazebnik YA, et al. Cleavage of lamin A by Mch2 alpha but not CPP32: multiple interleukin 1 beta-converting enzyme-related proteases with distinct substrate recognition properties are active in apoptosis. *Proc Natl Acad Sci USA* **1996**;93:8395–400.
- Slee EA, Harte MT, Kluck RM, et al. Ordering the cytochrome c-initiated caspase cascade: hierarchical activation of caspases-2, -3, -6, -7, -8, and -10 in a caspase-9-dependent manner. *J Cell Biol* **1999**;144:281–92.
- Chai F, Evdokiou A, Young GP, Zalewski PD. Involvement of p21^{Waf1/Cip1} and its cleavage by DEVD-caspase in apoptosis of colorectal cancer cells by dietary factor butyrate. *Carcinogenesis* **2000**;21:7–14.
- Donato N, Perez M. Tumor necrosis factor-induced apoptosis stimulates p53 accumulation and p21^{Waf1} proteolysis in ME-180 cells. *J Biol Chem* **1998**;273:5067–72.
- Levkau B, Koyama H, Raines EW, et al. Cleavage of p21^{Cip1/Waf1} and p27^{Kip1} mediates apoptosis in endothelial cells through activation of cdk2: role of a caspase cascade. *Molec Cell* **1998**;1:553–63.
- Gervais JL, Seth P, Zhang H. Cleavage of CDK inhibitor p21(Cip1/Waf1) by caspases is an early event during DNA damage-induced apoptosis. *J Biol Chem* **1998**;273:19207–12.
- O'Connor P. Mammalian G1 and G2 phase checkpoints. In: Kastan MB, ed. *Cancer surveys, checkpoint controls and cancer*. Vol 29. Cold Spring Harbor, NY: Cold Spring Harbor Laboratory Press, **1997**:151–82.
- Waga S, Stillman B. Cyclin-dependent kinase inhibitor p21 modulates the DNA primer-template recognition complex. *Mol Cell Biol* **1998**;18:4177–87.
- Medina V, Edmonds B, Young GP, James R, Appleton S, Zalewski PD. Induction of caspase-3 protease activity and apoptosis by butyrate and trichostatin A (inhibitors of histone deacetylase): dependence on protein synthesis and synergy with a mitochondrial/cytochrome c-dependent pathway. *Cancer Res* **1997**;57:3697–707.
- Zalewski PD, Forbes IJ, Betts WH. Correlation of apoptosis with change in intracellular labile Zn, using Zinquin, a new specific fluorescent probe for zinc. *Biochem J* **1993**;296:403–8.
- Mahadevan I, Kimber MC, Lincoln SF, et al. The synthesis of Zinquin ester and Zinquin acid, zinc (II)-specific fluorescing agents for use in the study of biological zinc (II). *Aust J Chem* **1996**;49:561–8.
- Teare JM, Islam R, Flanagan R, Gallagher S, Davies MG, Grabau C. Measurement of nucleic acid concentrations using the DyNA Quant and the GeneQuant. *Biotechniques* **1997**;22:1170–4.
- Mori H, Matsumoto Y, Tamada Y, Ohashi M. Apoptotic cell death in formation of vesicular skin lesions in patients with acquired zinc deficiency. *J Cutan Pathol* **1996**;23:359–63.
- Carey HV. Zinc deficiency and diarrhea: is uroguanylin the culprit? *Gastroenterology* **1998**;114:221–2.
- Chai F, Truong-Tran AQ, Ho LH, Zalewski PD. Regulation of caspase activation and apoptosis by cellular zinc fluxes and zinc deprivation: a review. *Immunol Cell Biol* **1999**;77:272–8.
- Truong-Tran A, Zalewski PD, Ruffin RE. Visualization of labile intracellular zinc and its role in apoptosis of primary ciliated airway epithelial cells and cell lines. *Am J Physiol* **2000** (in press).
- Krajewska M, Wang HG, Krajewski S, et al. Immunohistochemical analysis of in vivo patterns of expression of CPP32 (caspase-3), a cell death protease. *Cancer Res* **1997**;57:1605–13.
- Liu X, Kim CN, Pohl J, Wang X. Purification and characterization of an interleukin-1 β -converting enzyme family protease that activates cysteine protease P32 CPP32. *J Biol Chem* **1996**;271:13371–6.
- Wolf CM, Eastman A. The temporal relationship between protein phosphatase, mitochondrial cytochrome c release, and caspase activation in apoptosis. *Exp Cell Res* **1999**;247:505–13.
- Stennicke HR, Salvesen GS. Biochemical characteristics of caspases-3, -6, -7, and -8. *J Biol Chem* **1997**;272:25719–23.
- Fukamachi Y, Karasaki Y, Sugiura T, et al. Zinc suppresses apoptosis of U937 cells induced by hydrogen peroxide through an increase of the Bcl-2/Bax ratio. *Biochem Biophys Res Commun* **1998**;246:364–9.
- Cui L, Takagi Y, Wasa M, Sando K, Khan J, Okada A. Nitric oxide synthase inhibitor attenuates intestinal damage induced by zinc deficiency in rats. *J Nutr* **1999**;129:792–8.
- Blagosklonny MV, Wu GS, Omura S, el-Deiry WS. Proteasome-dependent regulation of p21WAF1/CIP1 expression. *Biochem Biophys Res Commun* **1996**;227:564–9.
- King KL, Cidlowski JA. Cell cycle regulation and apoptosis. *Annu Rev Physiol* **1998**;60:601–17.